HHS Public Access

Author manuscript

*Mol Cancer Ther*. Author manuscript; available in PMC 2022 April 01.

Published in final edited form as:

*Mol Cancer Ther*. 2021 October ; 20(10): 1893–1903. doi:10.1158/1535-7163.MCT-20-1017.

# Potent Synergistic Effect on c-Myc Driven Colorectal Cancers Using a Novel Indole-Substituted Quinoline with a Plk1 Inhibitor

**Yanqi Xie**[1,2], **Wen Zhang**[1,2], **Lichao Guo**[1,2,3], **Liliia M. Kril**[1,2,4], **Kristin L. Begley**[1,2,4], **Vitaliy M. Sviripa**[3,4], **Xi Chen**[1,2,3], **Xifu Liu**[3], **Eun Y. Lee**[2,5], **Daheng He**[2], **Chi Wang**[2], **Tianyan Gao**[1,2], **Xiaoqi Liu**[6], **B. Mark Evers**[2,7], **David S. Watt**[1,2,4,8,*], **Chunming Liu**[1,2,*]

[1]Department of Molecular and Cellular Biochemistry, College of Medicine, University of Kentucky, Lexington, KY 40536

[2]Lucille Parker Markey Cancer Center, University of Kentucky, Lexington, KY 40536

[3]Center for Drug Innovation and Discovery, Hebei Normal University, Shijiazhuang, Hebei 050024, People's Republic of China

[4]Center for Pharmaceutical Research and Innovation, College of Pharmacy, University of Kentucky, Lexington, KY 40536

[5]Department of Pathology &Laboratory Medicine, College of Medicine, University of Kentucky, Lexington, KY 40536

[6]Department of Toxicology and Cancer Biology, College of Medicine, University of Kentucky, Lexington, KY 40536

[7]Department of Surgery, College of Medicine, University of Kentucky, Lexington, KY 40536

[8]Department of Pharmaceutical Sciences, College of Pharmacy, University of Kentucky, Lexington, KY 40536

## Abstract

Developing effective treatments for colorectal cancers through combinations of small-molecule approaches and immunotherapies present intriguing possibilities for managing these otherwise intractable cancers. During a broad-based, screening effort against multiple colorectal cancer cell lines, we identified indole-substituted quinolines (ISQs), such as $N^7$,$N^7$-dimethyl-3-(1-methyl-1*H*-indol-3-yl)quinoline-2,7-diamine (ISQ-1), as potent *in vitro* inhibitors of several cancer cell lines. We found that ISQ-1 inhibited Wnt signaling, a main driver in the pathway governing colorectal cancer development, and ISQ-1 also activated adenosine monophosphate kinase (AMPK), a cellular energy-homeostasis master regulator. We explored the effect of ISQs on cell metabolism. Seahorse assays measuring oxygen consumption rate (OCR) indicated that ISQ-1 inhibited complex I (*i.e.*, NADH ubiquinone oxidoreductase) in the mitochondrial, electron transport chain (ETC). In addition, ISQ-1 treatment showed remarkable synergistic depletion of oncogenic c-Myc

*Correspondence to: chunming.liu@uky.edu or dwatt@uky.edu.

Conflict of Interest Statement

CL and WZ have partial ownership in a for-profit venture, Epionc, Inc., that seeks to develop small-molecule inhibitors for cancer treatment. In accord with University of Kentucky policies, this work was disclosed to the University of Kentucky's Intellectual Property Committee and to a Conflict-of-Interest Oversight Committee.

protein level *in vitro* and induced strong tumor remission *in vivo* when administered together with BI2536, a polo-like kinase-1 (Plk1) inhibitor. These studies point toward the potential value of dual drug therapies targeting the ETC and Plk-1 for the treatment of c-Myc-driven cancers.

## Introduction

Metabolic reprograming in tumors generates anabolic intermediates for the biosynthesis of lipids, carbohydrates, and nucleic acids that are necessary to promote tumor growth, and this reprogramming includes the well-known Warburg effect in which cancer cells up-regulate glycolysis. This glycolytic up-regulation is not, however, a consequence of the down-regulation of oxidative phosphorylation in cancer cells (1) that maintain their capacity to produce ATP through mitochondrial, oxidative phosphorylation (2–4). In fact, emerging evidence suggests that activation of oncogenes and inactivation of tumor suppressors promote mitochondrial biogenesis that drives tumorigenesis and maintains viable populations of cancer stem cells (5). Additional studies point to the up-regulation of genes in the oxidative phosphorylation pathway as an important part of the resistance mechanisms against therapeutic, antineoplastic agents (6–8). In a study that compared sixteen normal cell lines and thirty-one cancer cell lines, the average percentage contribution of oxidative phosphorylation to ATP production was well-matched: 83% for cancer cells and 80% for normal cells (9). In addition, 63% of rectal adenocarcinomas and 53% of colon adenocarcinomas harbor tumor-specific, nonsynonymous mutations in mitochondrial DNA (mtDNA) that encodes protein subunits of electron transport complexes I to V (10,11). Cancer cell lines with mtDNA-encoded mutations in complex I subunits were up to twenty-fold more sensitive to complex I inhibitors, such as metformin and phenformin, than the sensitivity of non-mutated complex I in normal cell lines (12). These linked observations that cancer cells retain functional oxidative phosphorylation machinery while driving metabolic reprogramming elsewhere suggest that the specific, simultaneous disruption of both pathways was a valid strategy for the development of colorectal cancer therapeutics.

The oncogenic transcriptional factors MYC proteins (c-Myc, n-Myc, l-Myc) are estimated to contribute to about 70% of all human cancers (13–15). Up-regulated MYC proteins, including c-Myc, drive tumorigenesis by promoting gene transcription, cellular metabolism, and cell proliferation (16–18). More than 90% of colorectal cancers are driven by an aberrant Wnt-β-catenin signaling pathway that upregulates Wnt-target genes including *MYC* (19). Pioneering studies that showed transient inactivation of MYC led to prolonged tumor remission in a conditional MYC-induced, transgenic, mouse tumor model (20). Systemic Myc inhibition in a Ras-induced lung cancer mouse model resulted in rapid tumor regression and reversible side-effects on normal regenerating tissues (21), a finding that demonstrated that MYC was a desirable therapeutic target in MYC-driven cancers. Although Myc was initially deemed as “undruggable” because it was an intrinsically disordered protein and lacked targetable, drug-binding pockets (22), direct and indirect pharmacological inhibitors of MYC emerged from studies with *in vitro* potencies in the micromolar concentration range (13,15,23,24). New agents and combination therapies with improved potency against MYC remain as an elusive but much needed therapy against colorectal cancers.

Our prior work revealed that a selective group of mitochondrial proton uncouplers that activated 5' adenosine monophosphate-activated protein kinase (AMPK), inhibited Wnt signaling, and reduced expression of Wnt signaling target genes including *MYC* (25). Metformin, best known as a low-potency ETC complex I inhibitor, reduced c-Myc *in vitro* and *in vivo* in certain prostate cancers (26). Phosphorylation of serine-62 in c-Myc by ERK or CDK kinases enhanced c-Myc stability, but the phosphorylation of c-Myc threonine-58 by GSK3β triggered serine-62 dephosphorylation by protein phosphatase 2A (PP2A), ubiquitination by the SCF-Fbw7 E3 ligase, and proteasomal destruction (13,27). Polo kinase-1 (Plk1) also effected the phosphorylation of c-Myc at serine-62 that in turn enhanced c-Myc stability in colorectal and breast cancers (28). Plk1 inhibitors, including BI2536 and volasertib, that is now in clinical trials (29), suppressed this undesired, growth-promoting c-Myc stabilization. These findings prompted our exploration of synergistic effects of reducing c-Myc stabilization in colorectal cancer through a combination of our newly identified ETC complex I and polo kinase-1 inhibitors.

## Materials and Methods

### Chemistry

**General Methods.—**Solvents and chemicals were used from commercial vendors without further purification unless otherwise noted. A published procedure (30) for the synthesis of substituted quinolines was used for the synthesis of ISQs. The synthesis of indole-substituted quinolines (ISQs) utilized 4-(*N,N*-dialkylamino-2-aminobenzaldehydes prepared by sequential nucleophilic aromatic substitution reactions of 4-fluoro-2-nitrobenzaldehyde with secondary amines and the subsequent reduction of the intermediate 4-dialkylamino-2-nitrobenzaldehydes with iron powder. A Friedländer condensation of these 4-(*N,N*-dialkylamino-2-aminobenzaldehydes with 2-(1-methyl-1*H*-indol-3-yl)acetonitrile, as described previously (30), secured the desired ISQs (Fig. 1A).

Nuclear magnetic resonance spectra were determined in dimethyl sulfoxide-$d_6$ (DMSO-$d_6$) using Varian instruments ($^1$H, 400; $^{13}$C, 100Mz). High resolution electrospray ionization (ESI) mass spectra were recorded using a LTQ-Orbitrap Velos mass spectrometer (Thermo Fisher Scientific, Waltham, MA, USA). The FT resolution was set at 100,000 (at 400 *m*/*z*). Samples were introduced through direct infusion using a syringe pump with a flow rate of 5 μL/min. Melting points were determined in open capillarity tubes with a Buchi B-535 apparatus and are uncorrected. Purity was established by combustion analyses performed by Atlantic Microlabs, Inc. (Norcross, GA). Detailed methods for chemical synthesis were included in the Supplementary Materials.

### Biology

#### Materials.

**Antibodies:** Axin2 (#2151, Cell signaling technology), c-Myc (#1472–1, Epitomics), β-actin (#A1978, Sigma), pACC (#11818, Cell signaling technology), Total ACC (#3676, Cell signaling technology), pAMPK (#2535, Cell signaling technology), Total AMPK (#2532, Cell signaling technology), GAPDH (#GTX627408, GeneTex), Plk1 (#sc-17783, Santa Cruz), cyclinD1 (#2978, Cell signaling technology), cyclinB1 (#4135, Cell signaling

technology), p-Akt (#9272, Cell signaling technology), Total-Akt (#1081–1, Epitomics), p-P70S6K (#9234, Cell signaling technology), Total-P70S6K (#2708, Cell signaling technology), p-4E-BP1 (#2855, Cell signaling technology), Total-4E-BP1 (#GTX109162, GeneTex), p-CDC2 (#9111, Cell signaling technology), Total-CDC2 (#GTX108120, GeneTex). Compounds: GSK461364 was purchased from Cayman Chemical (Ann Arbor, MI, USA). BI2536 was from Achemblock (Burlingame, CA). DAPI and PI were from ThermoFisher (Waltham, MA).

**Cell lines and cell culture—**LS174T cell line (LS174T-TR4) is a gift from Professor Hans Clevers and Marc van de Wetering. LS174T-TR4 cells were selected with resistance to blasticidin (31). PC3 and Beas-2B cells are obtained from Professor Vivek Rangnekar and have been authenticated for previous publications (32). SK-LMS-1 and HepG2 cells were purchased from American Type Culture Collection (ATCC) in 2019. *Mycoplasma* testing was performed using a sensitive PCR-based mycoplasma detection kit covering more than 200 species/strains of mycoplasmas (Biovision, K1476–100), and no mycoplasma contamination was found in the cell lines used in this work. All cells were cultured in the media recommended by ATCC at 37 °C with 5% $CO_2$ atmosphere in a water jacketed incubator (NuAire, Plymouth, MN).

**Western blotting—**Western blotting were performed according to previous procedures (25). Cells were split into 12-well plates. After 24 hours, compounds at indicated final concentrations were added to each well for another 24 hours unless otherwise noted. DMSO was used as a control. Cells were lysed in the appropriate volume of lysis buffer: 50 mM HEPES, 100 mM NaCl, 2 mM EDTA, 1% (v/v) glycerol, 50 mM NaF, 1 mM $Na_3VO_4$, 1% (v/v) Triton X-100, with protease inhibitors. Cell lysates were centrifuged, and supernatants were mixed with 6x protein loading buffer and boiled. The obtained samples were analyzed with standard western blotting methods with indicated antibodies.

**Cell proliferation inhibition assay—**Cell proliferation inhibition assays were done following a previous report (33). Cancer cells were seeded into 24-well plates at a density of 20,000 cells per well in 1 mL of culture medium and were cultured overnight at 37 °C. Compounds and the vehicle control (DMSO) were added to the cells. After 5 days, the medium was removed, and 100 μL of trypsin was added. The cells were re-suspended in phosphate-buffered saline (PBS) and were counted by Vi-CELL XR 2.03 (Beckman Coulter, Inc. USA). The ratio R of the number of viable cells in the compound treatment group to the number of viable cells in DMSO treatment group was taken as relative growth, and the percentage growth inhibition was calculated as (1-R) * 100.

**Reporter assay—**Wnt reporter assay was described previously (25). We subcloned Super 8xTOPFlash (provided by Professor Randall Moon, University of Washington) into the pGL4.83 [hRlucP/Puro] Vector and transfected it into HEK293T cells. A stable HEK293T cell line containing the TOPFlash reporter was established using puromycin selection (25). To assess if compounds of interest blocked the downstream signaling transduction pathway of β-catenin, the stable reporter cells were seeded to a 12-well plate and treated with 25 mM LiCl to stabilize β-catenin for 16 hours to activate Wnt signaling and then candidate

compounds at predetermined concentrations for another 24 hours. The cells were lysed and centrifuged to obtain supernatants which were analyzed by FB 12 Single Tube Luminometer by Titertek-Berthold (Berthold Detection Systems GmbH, Elsässerstr, Germany).

**Seahorse assay—**Seahorse assays were carried out following a published procedure (25). Briefly, $2.5 \times 10^4$ cells in 80 μL of medium were seeded in XF96 Cell Culture microplate for all experiments. On the next day, cell culture media were replaced with Seahorse XF modified media. Cells were treated with 1 μM of oligomycin A, 1.0 μM FCCP and mixture of 1.0 μM of rotenone and 1.0 μM of antimycin A in standard mitochondrial stress test conditions. To determine the uncoupler effects, FCCP was replaced with an equal volume of DMSO, or a compound to be tested in DMSO solution. To test whether compounds inhibited ETC complex V, oligomycin was replaced with an equal volume of DMSO, or compounds in DMSO solution. To assess if compounds inhibited ETC complex I or III, rotenone and antimycin A were replaced with an equal volume of DMSO, or compounds in DMSO solution.

**Mitochondrial ETC complex activity measurements using PMP—**Mitochondrial ETC complex activity measurements were taken using the Agilent Seahorse Assay with XF PMP (Agilent, Santa Clara, CA) following manufacturer's instructions. Adherent monolayer cells were gently washed with mitochondrial assay solution (MAS) (220 mM mannitol, 70 mM sucrose, 10 mM $KH_2PO_4$, 5 mM $MgCl_2$, 2 mM HEPES, 1 mM EGTA, and 0.2% (w/v) fatty acid free BSA) and cell growth media was replaced with MAS supplemented with 4mM adenosine diphosphate (ADP), 10 mM pyruvate, and 1 nM PMP. Following calibration, the assay was immediately performed by measuring baseline with two cycles of 0.5 min mixing, 0.5 min waiting, and 2 min measuring. After baseline measurements, sequential injections of DMSO, compounds of interest or 2 μM rotenone, 10 mM succinate, 2 μM antimycin A, and a combination of 10 mM ascorbate and 100 μM TMPD were also performed with each followed by two cycles of 0.5 min mixing, 0.5 min waiting, and 2 min measuring. Data were then normalized to cell counts using the Biotek Cytation 1 (BioTek Instruments, Winooski, VT, USA).

**Calculation of synergy scores of ISQ-1 and BI2536—**Cell proliferation inhibition assays described above were carried out using LS174T cells to evaluate the inhibitory effects of ISQ-1 with or without BI2536 at predetermined concentrations. The final treatment concentrations of ISQ-1 were 0 nM, 50 nM, 100 nM, 200 nM, 300 nM, and 400 nM in the presence or absence of BI2536 at 0 nM, 1 nM, 1.5 nM, 3 nM, 4.5 nM and 6 nM. Synergy scores were calculated using SynergyFinder web application (Version 2.0) at default parameters with Bliss as the reference model (34).

**Cell cycle analysis by flow cytometry—**Cell cycle analysis by flow cytometry was done following a previous report (33). Briefly, a million of LS174T cells were placed in 6-cm dishes and cultured at 37°C for 24 hours. DMSO or compounds in DMSO were added to the cells and incubated for additional 24 hours. The cells were trypsinized, washed with ice cold PBS twice, and resuspended in 500 μL of PBS. This cell suspension was added to 5 mL of 70% ethanol dropwise in a 15 mL tube that was placed on vortex and kept at

−20 °C overnight. The cells were further washed with PBS and 2 μL of 50 mg/ml RNase (final 0.2 mg/ml) and 2.5 μL of 4 mg/mL PI (final 20 μg/mL) were added. The mixture was incubated at dark for 45 min and filtered through 35 μm nylon mesh for analysis by the Flow Cytometry and Cell Sorting Shared Resource Facility of the University of Kentucky Markey Cancer Center.

**Colon Cancer Organoids—**The colon cancer organoids were isolated from $Apc^{f/+}$/$Kras^{LSL\text{-}G12D}$/Villin-Cre mouse model (35). Using 48-well drug screening to assess how compounds affected organoid colony formation, the Matrigel containing organoids was digested by 300 μL dispase. The gel was removed by 1,000 × 5 min spinning. The organoids were digested into single cells by 1 mL Trypsin and washed with 10 mL of ADF12. For each well, 80 μL of Matrigel was added to the bottom and 1000 cells in 60 μL Matrigel were added to the top. The cells were cultured in 250 μL of 3D complete medium (Advanced DMEM/F12 supplemented with 1 × N-2, 1 × B-27, 1 mM N-acetylcysteine and 1% penicillin/streptomycin). The cells were treated with DMSO or testing compounds and total number of organoids with diameter greater than 50 μm were analyzed and manually counted using microscope.

To evaluate whether compounds inhibited organoid growth, above procedures were followed and 10,000 single cells/ per well were plated in 24-well plate. After 3 days when organoids formed, fresh culture media were supplied, and compounds were added for additional 3 days. Organoid viability was measured using CellTiter-Glo® 3D Cell Viability Assay (Promega) following manufacturer's protocol.

***In vivo* evaluation of antineoplastic activity and gross toxicity in LS174T xenografts—**Mouse studies were carried out with approval from the Institutional Animal Care and Use Committee of the University of Kentucky (2020–3531). All methods were performed in accordance with the relevant guidelines and regulations according to protocols. LS174T cells suspended in 50% Matrigel (Corning, Glendale, Arizona) were subcutaneously injected in the lower flanks of severe combined immunodeficient mice (12 male mice and 8 female mice) at a density of $1 \times 10^6$ cells in 100 μL of 50% Matrigel. After tumors were established, mice were randomized according to tumor volume and divided into groups for treatments (five mice in each group, two tumors on each mouse).

The *in vivo* evaluation of ISQ-1 and BI2536 followed the approved protocol. After tumors were established, ISQ-1 was formulated in a mixture of Tween-80 (5%), DMSO (10%), PEG400 (25%) and PBS (60%) and was intraperitoneally administered to the ISQ-1 group at a daily dose of 20 mg/kg mouse body weight. The first day of treatment was set as day 0. At days 0, 4, and 7, BI2536 dissolved in 0.1 N HCl and then diluted 5-fold using 0.9% NaCl was given *via* gavage to the BI2536 group. Mice in combination therapy group were treated with both ISQ-1 and BI2536 following aforementioned dosing schedules. At day 11 treatment was ceased and mice were sacrificed. Tumors and mouse weights were measured, and tumor volumes were calculated as Length × $\text{width}^2/2$.

**Statistics—**Major biological assays were performed at least twice. Data were shown as mean ± SEM. For the mice study, five mice with two tumors on the lower flanks of each

mouse were used in each treatment group. Sizes of the two tumors from each mouse were averaged, standardized by the tumor size on day 0, and log-transformed. ANOVA with Tukey's HSD test was used to compare the tumor size at the end of the study (day 11) between the combination therapy of ISQ-1 and BI2536 and each single compound as well as the control. The equal variance assumption of ANOVA was assessed by Bartlett's test. All statistical studies were overseen in collaboration with a statistician in the University of Kentucky's Markey Cancer Center.

## Results

Deregulated Wnt signaling is the main driver of colorectal cancer initiation and progression. Our long-standing efforts to develop drug candidates for the treatment of colorectal cancers (30,33,36–38) focused on the Wnt pathway and led to a family of aryl-substituted quinolines called "arylquins". Using a combination of a Wnt reporter assay and an AMPK activation assay, we identified indole-substituted quinolines (ISQs) bearing C-3 *N*-methylindole groups, such as $N^7$,$N^7$-dimethyl-3-(1-methyl-1*H*-indol-3-yl)quinoline-2,7-diamine (ISQ-1) (Fig. 1A), that inhibited *in vitro* cell growth of colon cancer LS174T, prostate cancer PC-3, sarcoma SK-LMS-1 and liver cancer HepG2 cell lines at nanomolar concentrations (Fig. 1B). We found that ISQ-1 also inhibited Wnt signaling target genes including c-Myc and axin2 and activated AMPK in a dose-dependent manner (Figs. 1C–1E). The synthesis and structural characterization of ISQs are described in Materials and Methods section.

A study of structure-activity relationships (SAR) using cell proliferation assays as a readout quickly revealed the importance of the *N*,*N*-dialkylamino group at C-7 in the ISQ pharmacophore (*i.e.*, R in Fig. S1), an amino group at C-2 and an *N*-methyl-3-indolyl group at C-3. The substitution of other aryl or heteroaryl groups for the *N*-methyl-3-indolyl group in ISQs were unrewarding in terms of identifying inhibitors with $IC_{50}$ values less than 100 nM. Variations, however, at the C-7 position in the ISQs produced a series of important inhibitors. Initial studies of the percentage inhibition of LS174T cell proliferation at 500 nM, as shown in Table S1, indicated that ISQs bearing a simple *N*,*N*-dimethylamino group at C-7 (*i.e.*, ISQ-1) were more active than those bearing *N*-piperidinyl (*i.e.*, ISQ-2), *N*-alkylpiperazinyl (*i.e.*, ISQ-3, 4 and 5) or *N*-phenylpiperazinyl groups (*i.e.*, ISQ-6). In contrast, however, ISQs bearing additional oxygen or nitrogen atoms in N-alkylpiperazinyl groups, as in the *N*-cyano, *N*-hydroxymethyl or *N*-methoxymethylpiperazinyl analogs (ISQ-7, 8 and 9, respectively) or an additional nitrogen atom in the *N*-arylpiperazinyl group, as in *N*-(4-pyridyl)piperazinyl analog (ISQ-10) possessed inhibitory activity comparable to the *N*,*N*-dimethylamino group in ISQ-1 at 500 nM. Dose response studies for these ISQs as inhibitors in these cell proliferation assays revealed that the most promising of these ISQ inhibitors with $IC_{50}$ values in the 100 nM range were those in which the piperazinyl group at C-3 possessed heteroatom-substituted groups (*i.e.*, ISQ-7, 8, 9 and 10).

Our previous work revealed that certain mitochondrial proton uncouplers that activated AMPK also inhibited Wnt signaling by disrupting energy supply for signaling transduction (25). The dual effects of ISQs on Wnt signaling and AMPK activation prompted an investigation of the effects of ISQs on oxidative phosphorylation using Agilent Seahorse assays. We initially compared known uncoupler *N*-(4-

(trifluoromethoxy)phenyl)carbonohydrazonoyl dicyanide (FCCP) with ISQ-1 in dimethyl sulfoxide (DMSO) or the vehicle alone in a standard Seahorse assay. Unlike known mitochondrial proton uncouplers such as FCCP that activated AMPK (25), ISQ-1 failed to rescue oligomycin-inhibited oxygen consumption rate (OCR) and thus was not a mitochondrial proton uncoupler (Figs. 2A, S2).

We next determined if ISQ-1 inhibited protein complexes in the electron transport chain (ETC). We compared the effects of oligomycin, a known mitochondrial complex V/ATP synthase inhibitor, with ISQ-1 in DMSO or with vehicle alone. As expected, oligomycin suppressed ATP-linked respiration and decreased OCR followed by an increased OCR upon the addition of FCCP that collapsed the inner membrane gradient and drove the ETC to function to its maximal rate (Figs. 2B, S3). In contrast, in the presence of ISQ-1, the decreased OCR could not be “rescued” by the addition of FCCP (Figs. 2B, S3), an outcome suggesting that ISQ-1 did not inhibit mitochondrial complex V. We next replaced antimycin A, a complex III inhibitor, and rotenone, a complex I inhibitor with ISQ-1 in DMSO or vehicle alone in the Seahorse assay and found that ISQ-1 suppressed OCR to an extent that was similar to that of rotenone or antimycin (Figs. 2C, S4), implying that it inhibited either complex I or complex III of the ETC.

To reveal the precise mechanism by which ISQ-1 affected mitochondria, we measured substrate specific ETC/oxidative phosphorylation activity with or without the addition of ISQ-1 or known ETC complex inhibitors using plasma membrane permeabilizer (PMP)-treated cells (39). PMP is a bacterial recombinant cholesterol-dependent cytolysin that forms pores on plasma membranes while sparing mitochondrial membranes (40). These pores on plasma membranes facilitate the passage of solutes and small proteins and thereby allow the control of ETC complex-specific substrate/inhibitor provision. Permeabilized cells were given pyruvate, a complex I-linked substrate, followed by the addition of DMSO, and either the complex I inhibitor, rotenone, or ISQ-1. Surprisingly, we noted that ISQ-1 halted pyruvate/NADH-linked respiration in a dose-dependent manner relative to DMSO alone (Fig. 2D). This effect was mimicked by the complex I inhibitor, rotenone, to a similar degree, and this outcome suggested that ISQ-1 was a complex I inhibitor. Next, succinate was added to drive respiration from electrons that were fed directly into the ubiquinone pool by succinate dehydrogenase (complex II) that by-passed complex I inhibition. Both rotenone-treated and ISQ-1-treated permeabilized cells showed increased respiration (Fig. 2D), an outcome that ruled out the possibility that ISQ-1 inhibited complexes II, III, or IV. As anticipated, the subsequent addition of complex III inhibitor, antimycin A, abolished OCR but this abolition was “rescued” by the injection of a complex III electron donor, *N,N,N,N*-tetramethyl-p-phenylenediamine (TMPD) (Fig. 2D), essentially by-passing the blockade at complex III and delivering electrons directly to cytochrome c oxidase (complex IV). In summary, the Seahorse assay data using ETC complex-specific inhibitors and PMP-permeabilized cells demonstrated that ISQ-1 inhibited complex I, disrupted mitochondrial function, activated AMPK, and inhibited Wnt signaling. Similar results were obtained for ISQ-7, a more potent analog of ISQ-1 (Fig. S1, Table S1). Seahorse assays showed that ISQ-7 inhibited complex I or III (Figs. S4, S5A) and mitochondrial ETC complex activity measurements on permeabilized cells by PMP further revealed that ISQ-7 inhibited complex

I (Fig. S5B). In a fashion similar to ISQ-1, ISQ-7 strongly inhibited Wnt target genes, Axin-2 and c-Myc (Fig. S5C) and activated AMPK (Fig. S5D) in a dose-dependent manner.

To understand the mechanisms of ISQs and to identify other drugs with potential lethal effects in combination with ISQs, we analyzed the effects on ISQs on several cell signaling pathways (Fig. 3A). Perhaps not unexpectedly, these compounds inhibited the expression and activation of Wnt and mTOR signaling and affected cell cycle progression, consistent with their function as mitochondrial complex I inhibitors that altered ATP levels. Surprisingly, however, we found that a key cell cycle regulator, Plk1, was upregulated by ISQs (Fig. 3A). Plk1, a well-known oncoprotein, is highly overexpressed in human colorectal tumors compared with adjacent normal tissues (28). Plk1 is required for cell cycle progression and its expression is associated with drug resistance. More importantly, Plk1 promoted the phosphorylation of c-Myc at serine-62 that enhanced c-Myc stability in colorectal cancer and breast cancer (28), and Plk1 inhibitor BI2536 suppressed this oncogenic c-Myc stabilization. Because ISQs reduced c-Myc levels through inhibiting Wnt signaling, we explored whether ISQs possessed synergistic effects with BI2536 with respect to c-Myc levels. Co-treatment of LS174T cells with the combination of either ISQ-1 or ISQ-7 and with BI2536 for 24 hours led to synergistic reduction of c-Myc levels compared with the effects of either ISQ-1 or ISQ-7 when used alone (Fig. 3B). To validate these results, we repeated this experiment with another well-characterized Plk1 inhibitor, GSK461364, that has been approved for clinical trials. Similar to BI2536, GSK461364 synergized with ISQ-1 or ISQ-7 on c-Myc inhibition (Fig. 3C). Similar results were obtained in prostate cancer PC3 cells (Fig. 3D). We also analyzed the effects of ISQ-1 and BI2536 on cell cycle of LS174T colorectal cancer cells. The combination of these two compounds synergistically inhibited the G2/M transition (Fig. 4A). To confirm that the relationship between ISQ-1 and BI2536 was synergistic rather than additive, we calculated synergy scores using SynergyFinder web application (Version 2.0) at default parameters with Bliss as the reference model (34). We found that the average synergy score was > 10 and at certain concentrations (ISQ-1 100–300 nM and BI2536 1.5–4.5 nM) the corresponding synergy score was > 15 (Fig. 4B), indicating that ISQ-1 indeed synergized with BI2536 (34). Collectively, these data provided a rationale for further evaluation of ISQs in combination with Plk1 inhibitors.

Although ISQ-1 was less potent than ISQ-7 *in vitro*, its solubility was better than that of ISQ-7. We evaluated ISQ-1 using a more pathologically relevant, 3D-tumor organoid model established from $Apc^{f/+}/Kras^{LSL\text{-}G12D}$/Vil-Cre compound mutant mouse (35,41). ISQ-1 inhibited tumor organoid formation from single cells (Figs. 5A, 5B) and inhibited organoid growth in a dose-dependent manner (Fig. 5C), a finding that prompted us to explore the *in vivo* therapeutic efficiencies of ISQ-1 and its combination with a Plk-1 inhibitor. A colon cancer xenograft model established from LS174T cells in nude mice was used to assess the *in vivo* tumor inhibitory potential of the ISQ-1 and Plk1 inhibitor BI2536. Daily dosing of ISQ-1 at 20 mg/kg body weight daily or BI2536 at 30 mg/kg body weight twice a week inhibited tumor growth but did not induce tumor regression (Figs. 6A, 6B). The combination therapy of ISQ-1 and BI2536 resulted in significant tumor remission (Figs. 6A, 6B) relative to either compound used alone. No gross toxicities were observed on the basis of mouse weight measurements (Fig. 6C). Tumor sections were analyzed with H&E and

Ki-67 staining (Figs. 6D, 6E). The tumors displayed poorly differentiated carcinomas with pleomorphism and brisk mitotic activity. The tumors treated with a combination of ISQ-1 and BI2536 were more pleomorphic (*i.e.*, large nuclei, prominent nucleoli, considerable variation in nuclear size, etc.) than that those treated with individual compounds (Fig. 6E). The combination treatment with ISQ-1 and BI2536 was more effective in inhibiting tumor proliferation (Fig. 6E) than either agent alone.

## Discussion

Building on our long-standing efforts to identify and develop potential drug candidates for cancer treatment (25,30,33,36–38,42,43), we discovered Wnt signaling inhibitors featuring an indole-substituted, quinoline scaffold called ISQs. A representative compound, namely ISQ-1 (Fig. 1A), possessed nanomolar potencies towards inhibiting Wnt signaling and cell proliferation in multiple tumor cell lines. A series of Agilent Seahorse assays and mitochondrial ETC complex activity measurements using PMP-permeabilized cells revealed that ISQ-1 and ISQ-7 were not mitochondrial proton uncouplers but rather mitochondrial ETC complex I inhibitors. Mechanistically, ISQs inhibited mitochondrial complex I, disrupted mitochondrial respiration function, reduced energy supply for signaling transduction, and thus inhibited aberrantly active Wnt-β-catenin signaling that contributed to cell proliferation in more than 90% of colorectal cancers. Recent studies indicated that a majority of tumor cells, particularly cancer stem cells, depended on oxidative phosphorylation for ATP production (2–4). In comparison with normal cells, colorectal cancers often harbor tumor-specific, nonsynonymous mutations or copy-number alterations in mitochondrial DNA (mtDNA) that render them more sensitive to less potent complex I inhibitors (10–12) and that also confer ISQs selectivity toward colorectal cancer cells over healthy cells. Although ISQ-1 also inhibited mitochondrial oxidative phosphorylation in normal epithelial cells (Beas-2B) (Figs. S2-S4), it was less active in activating AMPK signaling in normal cells (Fig. S6) than it was in cancer cells (Fig. 1E), an observation that confirmed selectivity of ISQs for cancer cells over normal cells.

A growing body of evidence connects mitochondrial oxidative phosphorylation with drug resistance in multiple cancer types. A subset of diffuse, large B cell lymphoma cells escaped from inhibition of B cell receptor (BCR) survival signals and persisted because of enhanced mitochondrial function (44). Increased mitochondrial metabolism through Pgc1α/c-Myc-mediated transcriptional regulation pathways also played a role in exacerbated growth and chemotherapy resistance in melanoma and in triple-negative breast cancer (45,46). Mutations in the subunit gene, Smarca4, of the SWI/SNF chromatin remodeling complex led to dependence of Smarca4-deficient lung tumors on elevated oxidative phosphorylation (47,48). Kinase inhibitors, such the EGFR inhibitor, gefitinib, and the BRAF V600E inhibitor, vemurafenib, induced enhanced mitochondrial metabolism and drug resistance (49–51). These drug-resistance cases highlight the potential use of ISQs for targeting oxidative phosphorylation as a therapeutic opportunity in multiple well-defined refractory cancers and provides an approach for overcoming certain types of drug resistance.

*MYC*, a master regulator of cell cycle and proliferative glycolysis, is a well-established Wnt signaling target gene, and the encoded MYC proteins present formidable challenges

for pharmacological targeting (16,22). We found that ISQs decreased c-Myc protein levels in colon cancer cell line LS174T. This c-Myc reduction was accompanied by unexpected increase of Plk1 (Fig. 3A), another positive cell cycle regulator (52). In neural cancers, Plk1 indirectly increased n-Myc by phosphorylating SCF-Fbw7 E3 ubiquitin ligase and inducing its proteasomal degradation that counteracted SCF-Fbw7-mediated degradation of n-Myc (53). In colorectal cancer and breast cancer, Plk1 promoted the phosphorylation of c-Myc at serine-62 that enhanced c-Myc stability (28). ISQ-1 treatment reduced c-Myc in LS174T cells, and this effect was blocked by proteasome inhibitor MG132 and enhanced by protein translation inhibitor cycloheximide (CHX) (Fig. S7), outcomes that suggested that ISQ-1 regulated c-Myc at multiple levels. We observed that ISQ-1 induced both Plk-1 and cyclin B1 in colon cancer cells (Fig. 3A). Cooperation of Plk1 and Cyclin B1 plays an essential role in G2/M transition (54) that may lead to resistance to ISQs treatment. Based on these data, we developed a combination therapy of ISQs and Plk1 inhibitor BI2536 which achieved remarkable synergistic reduction of c-MYC expression and cell cycle progression *in vitro* and tumor remission *in vivo*.

Although BI2536 proved to be safe in phase I clinical trials, it displayed only limited antitumor activity in Phase II clinical trials(55). ISQ-1 significantly enhanced the efficacies of BI2536 both *in vitro* (Fig. 4) and *in vivo* (Fig. 6) and suggested that ISQs and Plk1 inhibitors could provide effective combinational therapies. In this study, we focused on c-Myc regulation by ISQs and Plk1 inhibitors. However, these inhibitors may have synergistic effects on other cancer targets as well. In addition, ISQs may also enhance the efficacy of the other therapeutic agents. For example, cancer immunotherapy has revolutionized cancer treatment and a small portion of patients show complete tumor remission after immune checkpoint blockade therapies. *MYC* has been shown to regulate immune checkpoint molecule PD-L1 (56) and cooperates with Ras to induce an immune suppressive tumor microenvironment to drive tumorigenesis (57). Recently, a small molecule MYC inhibitor, called MYCi361, induced immunogenic cell death (ICD), modulated antitumor tumor immune microenvironment, and synergized with immune checkpoint blockade therapy (58). We envision that our newly identified ISQs in combination with Plk1 inhibition would not only support an effective combination approach of pharmacological targeting c-Myc driven cancers but also highlight the potential of synergizing with immune checkpoint blockade therapies to eradicate refractory “MYC-addicted” cancers.

## Supplementary Material

Refer to Web version on PubMed Central for supplementary material.

## Acknowledgments

CL and DSW were supported by NIH R01 CA172379 from the National Institutes of Health and by NIH UL1 TR000117 from the National Institutes of Health to the University of Kentucky’s Center for Clinical and Translational Science and by Markey Cancer Center Alliance Award. DSW was also supported in part by the Office of the Dean of the College of Medicine, the Center for Pharmaceutical Research and Innovation in the College of Pharmacy, the Department of Defense (DoD Prostate Cancer Research Program Award W81XWH-16-1-0635 [Grant Log# PC150326P2]), and NIH P30 RR020171 from the National Institute of General Medical Sciences to L. Hersh. VMS was supported by grant IRG 16-182-28 from the American Cancer Society). This research was supported by Biostatistics & Bioinformatics Shared Resource Facility (BB SRF), the Biospecimen Procurement and

Translational Pathology Shared Resource Facility (BPTP SRF) and the Redox Metabolism Shared Resource Facility (RM SRF) of the University of Kentucky Markey Cancer Center (P30CA177558).

## References


1. Ashton TM, McKenna WG, Kunz-Schughart LA, Higgins GS. Oxidative Phosphorylation as an Emerging Target in Cancer Therapy. Clin Cancer Res2018;24(11):2482–90 doi 10.1158/1078-0432.CCR-17-3070. [PubMed: 29420223]
2. Weinberg SE, Chandel NS. Targeting mitochondria metabolism for cancer therapy. Nat Chem Biol2015;11(1):9–15 doi 10.1038/nchembio.1712. [PubMed: 25517383]
3. Chandel NS. Mitochondria as signaling organelles. BMC Biol2014;12:34 doi 10.1186/1741-7007-12-34. [PubMed: 24884669]
4. DeBerardinis RJ, Chandel NS. Fundamentals of cancer metabolism. Sci Adv2016;2(5):e1600200 doi 10.1126/sciadv.1600200. [PubMed: 27386546]
5. Vyas S, Zaganjor E, Haigis MC. Mitochondria and Cancer. Cell2016;166(3):555–66 doi 10.1016/j.cell.2016.07.002. [PubMed: 27471965]
6. Wolf DA. Is reliance on mitochondrial respiration a “chink in the armor” of therapy-resistant cancer?Cancer cell2014;26(6):788–95 doi 10.1016/j.ccell.2014.10.001. [PubMed: 25490445]
7. Zhang G, Frederick DT, Wu L, Wei Z, Krepler C, Srinivasan S, et al. Targeting mitochondrial biogenesis to overcome drug resistance to MAPK inhibitors. J Clin Invest2016;126(5):1834–56 doi 10.1172/JCI82661. [PubMed: 27043285]
8. Roesch A, Vultur A, Bogeski I, Wang H, Zimmermann KM, Speicher D, et al. Overcoming intrinsic multidrug resistance in melanoma by blocking the mitochondrial respiratory chain of slow-cycling JARID1B(high) cells. Cancer cell2013;23(6):811–25 doi 10.1016/j.ccr.2013.05.003. [PubMed: 23764003]
9. Zu XL, Guppy M. Cancer metabolism: facts, fantasy, and fiction. Biochem Biophys Res Commun2004;313(3):459–65 doi 10.1016/j.bbrc.2003.11.136. [PubMed: 14697210]
10. Larman TC, DePalma SR, Hadjipanayis AG, Cancer Genome Atlas Research N, Protopopov A, Zhang J, et al. Spectrum of somatic mitochondrial mutations in five cancers. Proc Natl Acad Sci U S A2012;109(35):14087–91 doi 10.1073/pnas.1211502109. [PubMed: 22891333]
11. Yu M, Generation function and diagnostic value of mitochondrial DNA copy number alterations in human cancers. Life Sci2011;89(3–4):65–71 doi 10.1016/j.lfs.2011.05.010. [PubMed: 21683715]
12. Birsoy K, Possemato R, Lorbeer FK, Bayraktar EC, Thiru P, Yucel B, et al. Metabolic determinants of cancer cell sensitivity to glucose limitation and biguanides. Nature2014;508(7494):108–12 doi 10.1038/nature13110. [PubMed: 24670634]
13. Dang CV. MYC on the path to cancer. Cell2012;149(1):22–35 doi 10.1016/j.cell.2012.03.003. [PubMed: 22464321]
14. Kalkat M, De Melo J, Hickman KA, Lourenco C, Redel C, Resetca D, et al. MYC Deregulation in Primary Human Cancers. Genes (Basel)2017;8(6) doi 10.3390/genes8060151.
15. Carabet LA, Rennie PS, Cherkasov A. Therapeutic Inhibition of Myc in Cancer. Structural Bases and Computer-Aided Drug Discovery Approaches. Int J Mol Sci2018;20(1) doi 10.3390/ijms20010120.
16. Dang CV. MYC, metabolism, cell growth, and tumorigenesis. Cold Spring Harb Perspect Med2013;3(8) doi 10.1101/cshperspect.a014217.
17. Nesbit CE, Tersak JM, Prochownik EV. MYC oncogenes and human neoplastic disease. Oncogene1999;18(19):3004–16 doi 10.1038/sj.onc.1202746. [PubMed: 10378696]
18. Secombe J, Pierce SB, Eisenman RN. Myc: a weapon of mass destruction. Cell2004;117(2):153–6 doi 10.1016/s0092-8674(04)00336-8. [PubMed: 15084254]
19. Shi L, Wu YX, Yu JH, Chen X, Luo XJ, Yin YR. Research of the relationship between beta-catenin and c-myc-mediated Wnt pathway and laterally spreading tumors occurrence. Eur Rev Med Pharmacol Sci2017;21(2):252–7. [PubMed: 28165564]
20. Jain M, Arvanitis C, Chu K, Dewey W, Leonhardt E, Trinh M, et al. Sustained loss of a neoplastic phenotype by brief inactivation of MYC. Science2002;297(5578):102–4 doi 10.1126/science.1071489. [PubMed: 12098700]

21. Soucek L, Whitfield J, Martins CP, Finch AJ, Murphy DJ, Sodir NM, et al. Modelling Myc inhibition as a cancer therapy. Nature2008;455(7213):679–83 doi 10.1038/nature07260. [PubMed: 18716624]
22. Horiuchi D, Anderton B, Goga A. Taking on challenging targets: making MYC druggable. Am Soc Clin Oncol Educ Book2014:e497–502 doi 10.14694/EdBook_AM.2014.34.e497. [PubMed: 24857145]
23. Wolf E, Eilers M. Targeting MYC Proteins for Tumor Therapy. Annual Review of Cancer Biology2020;4(1):61–75 doi 10.1146/annurev-cancerbio-030518-055826.
24. Chen H, Liu H, Qing G. Targeting oncogenic Myc as a strategy for cancer treatment. Signal Transduct Target Ther2018;3:5 doi 10.1038/s41392-018-0008-7. [PubMed: 29527331]
25. Zhang W, Sviripa VM, Kril LM, Yu T, Xie Y, Hubbard WB, et al. An Underlying Mechanism of Dual Wnt Inhibition and AMPK Activation: Mitochondrial Uncouplers Masquerading as Wnt Inhibitors. J Med Chem2019;62(24):11348–58 doi 10.1021/acs.jmedchem.9b01685. [PubMed: 31774672]
26. Akinyeke T, Matsumura S, Wang X, Wu Y, Schalfer ED, Saxena A, et al. Metformin targets c-MYC oncogene to prevent prostate cancer. Carcinogenesis2013;34(12):2823–32 doi 10.1093/carcin/bgt307. [PubMed: 24130167]
27. Welcker M, Orian A, Jin J, Grim JE, Harper JW, Eisenman RN, et al. The Fbw7 tumor suppressor regulates glycogen synthase kinase 3 phosphorylation-dependent c-Myc protein degradation. Proc Natl Acad Sci U S A2004;101(24):9085–90 doi 10.1073/pnas.0402770101. [PubMed: 15150404]
28. Tan J, Li Z, Lee PL, Guan P, Aau MY, Lee ST, et al. PDK1 signaling toward PLK1-MYC activation confers oncogenic transformation, tumor-initiating cell activation, and resistance to mTOR-targeted therapy. Cancer Discov2013;3(10):1156–71 doi 10.1158/2159-8290.CD-12-0595. [PubMed: 23887393]
29. Gutteridge RE, Ndiaye MA, Liu X, Ahmad N. Plk1 Inhibitors in Cancer Therapy: From Laboratory to Clinics. Mol Cancer Ther2016;15(7):1427–35 doi 10.1158/1535-7163.MCT-15-0897. [PubMed: 27330107]
30. Burikhanov R, Sviripa VM, Hebbar N, Zhang W, Layton WJ, Hamza A, et al. Arylquins target vimentin to trigger Par-4 secretion for tumor cell apoptosis. Nat Chem Biol2014;10(11):924–6 doi 10.1038/nchembio.1631. [PubMed: 25218743]
31. Barker N, Hurlstone A, Musisi H, Miles A, Bienz M, Clevers H. The chromatin remodelling factor Brg-1 interacts with beta-catenin to promote target gene activation. EMBO J2001;20(17):4935–43 doi 10.1093/emboj/20.17.4935. [PubMed: 11532957]
32. Hebbar N, Burikhanov R, Shukla N, Qiu S, Zhao Y, Elenitoba-Johnson KSJ, et al. A Naturally Generated Decoy of the Prostate Apoptosis Response-4 Protein Overcomes Therapy Resistance in Tumors. Cancer Res2017;77(15):4039–50 doi 10.1158/0008-5472.CAN-16-1970. [PubMed: 28625975]
33. Xie Y, Kril LM, Yu T, Zhang W, Frasinyuk MS, Bondarenko SP, et al. Semisynthetic aurones inhibit tubulin polymerization at the colchicine-binding site and repress PC-3 tumor xenografts in nude mice and myc-induced T-ALL in zebrafish. Sci Rep2019;9(1):6439 doi 10.1038/s41598-019-42917-0. [PubMed: 31015569]
34. Ianevski A, Giri AK, Aittokallio T. SynergyFinder 2.0: visual analytics of multi-drug combination synergies. Nucleic Acids Res2020;48(W1):W488–W93 doi 10.1093/nar/gkaa216. [PubMed: 32246720]
35. Wen YA, Xing X, Harris JW, Zaytseva YY, Mitov MI, Napier DL, et al. Adipocytes activate mitochondrial fatty acid oxidation and autophagy to promote tumor growth in colon cancer. Cell Death Dis2017;8(2):e2593 doi 10.1038/cddis.2017.21. [PubMed: 28151470]
36. Frasinyuk MS, Zhang W, Wyrebek P, Yu T, Xu X, Sviripa VM, et al. Developing antineoplastic agents that target peroxisomal enzymes: cytisine-linked isoflavonoids as inhibitors of hydroxysteroid 17-beta-dehydrogenase-4 (HSD17B4). Org Biomol Chem2017;15(36):7623–9 doi 10.1039/c7ob01584d. [PubMed: 28868548]
37. Zhang W, Sviripa V, Chen X, Shi J, Yu T, Hamza A, et al. Fluorinated N,N-dialkylaminostilbenes repress colon cancer by targeting methionine S-adenosyltransferase 2A. ACS Chem Biol2013;8(4):796–803 doi 10.1021/cb3005353. [PubMed: 23363077]

38. Zhang W, Sviripa V, Kril LM, Chen X, Yu T, Shi J, et al. Fluorinated N,N-dialkylaminostilbenes for Wnt pathway inhibition and colon cancer repression. J Med Chem2011;54(5):1288–97 doi 10.1021/jm101248v. [PubMed: 21291235]
39. Salabei JK, Gibb AA, Hill BG. Comprehensive measurement of respiratory activity in permeabilized cells using extracellular flux analysis. Nat Protoc2014;9(2):421–38 doi 10.1038/nprot.2014.018. [PubMed: 24457333]
40. Divakaruni AS, Wiley SE, Rogers GW, Andreyev AY, Petrosyan S, Loviscach M, et al. Thiazolidinediones are acute, specific inhibitors of the mitochondrial pyruvate carrier. Proc Natl Acad Sci U S A2013;110(14):5422–7 doi 10.1073/pnas.1303360110. [PubMed: 23513224]
41. Xiong X, Wen YA, Fairchild R, Zaytseva YY, Weiss HL, Evers BM, et al. Upregulation of CPT1A is essential for the tumor-promoting effect of adipocytes in colon cancer. Cell Death Dis2020;11(9):736 doi 10.1038/s41419-020-02936-6. [PubMed: 32913185]
42. Kril LM, Vilchez V, Jiang J, Turcios L, Chen C, Sviripa VM, et al. N-Aryl benzenesulfonamide inhibitors of [3H]-thymidine incorporation and beta-catenin signaling in human hepatocyte-derived Huh-7 carcinoma cells. Bioorg Med Chem Lett2015;25(18):3897–9 doi 10.1016/j.bmcl.2015.07.040. [PubMed: 26243371]
43. Zhang W, Sviripa V, Xie Y, Yu T, Haney M, Blackburn J, et al. Epigenetic Regulation of Wnt Signaling by Carboxamide-substituted Benzhydryl Amines That Function as Histone Demethylase Inhibitors. iScience2020;101795. [PubMed: 33305174]
44. Caro P, Kishan AU, Norberg E, Stanley IA, Chapuy B, Ficarro SB, et al. Metabolic signatures uncover distinct targets in molecular subsets of diffuse large B cell lymphoma. Cancer cell2012;22(4):547–60 doi 10.1016/j.ccr.2012.08.014. [PubMed: 23079663]
45. Vazquez F, Lim JH, Chim H, Bhalla K, Girnun G, Pierce K, et al. PGC1alpha expression defines a subset of human melanoma tumors with increased mitochondrial capacity and resistance to oxidative stress. Cancer cell2013;23(3):287–301 doi 10.1016/j.ccr.2012.11.020. [PubMed: 23416000]
46. Lee KM, Giltnane JM, Balko JM, Schwarz LJ, Guerrero-Zotano AL, Hutchinson KE, et al. MYC and MCL1 Cooperatively Promote Chemotherapy-Resistant Breast Cancer Stem Cells via Regulation of Mitochondrial Oxidative Phosphorylation. Cell Metab2017;26(4):633–47e7 doi 10.1016/j.cmet.2017.09.009. [PubMed: 28978427]
47. Lissanu Deribe Y, Sun Y, Terranova C, Khan F, Martinez-Ledesma J, Gay J, et al. Mutations in the SWI/SNF complex induce a targetable dependence on oxidative phosphorylation in lung cancer. Nat Med2018;24(7):1047–57 doi 10.1038/s41591-018-0019-5. [PubMed: 29892061]
48. Molina JR, Sun Y, Protopopova M, Gera S, Bandi M, Bristow C, et al. An inhibitor of oxidative phosphorylation exploits cancer vulnerability. Nat Med2018;24(7):1036–46 doi 10.1038/s41591-018-0052-4. [PubMed: 29892070]
49. Corazao-Rozas P, Guerreschi P, Jendoubi M, Andre F, Jonneaux A, Scalbert C, et al. Mitochondrial oxidative stress is the Achille's heel of melanoma cells resistant to Braf-mutant inhibitor. Oncotarget2013;4(11):1986–98 doi 10.18632/oncotarget.1420. [PubMed: 24161908]
50. Haq R, Shoag J, Andreu-Perez P, Yokoyama S, Edelman H, Rowe GC, et al. Oncogenic BRAF regulates oxidative metabolism via PGC1alpha and MITF. Cancer cell2013;23(3):302–15 doi 10.1016/j.ccr.2013.02.003. [PubMed: 23477830]
51. Takenaka T, Katayama M, Sugiyama A, Hagiwara M, Fujii I, Takatani-Nakase T, et al. Gefitinib Enhances Mitochondrial Biological Functions in NSCLCs with EGFR Mutations at a High Cell Density. Anticancer Res2017;37(9):4779–88 doi 10.21873/anticanres.11884. [PubMed: 28870896]
52. Gjertsen BT, Schoffski P. Discovery and development of the Polo-like kinase inhibitor volasertib in cancer therapy. Leukemia2015;29(1):11–9 doi 10.1038/leu.2014.222. [PubMed: 25027517]
53. Xiao D, Yue M, Su H, Ren P, Jiang J, Li F, et al. Polo-like Kinase-1 Regulates Myc Stabilization and Activates a Feedforward Circuit Promoting Tumor Cell Survival. Mol Cell2016;64(3):493–506 doi 10.1016/j.molcel.2016.09.016. [PubMed: 27773673]
54. Yuan J, Eckerdt F, Bereiter-Hahn J, Kurunci-Csacsko E, Kaufmann M, Strebhardt K. Cooperative phosphorylation including the activity of polo-like kinase 1 regulates the subcellular localization of cyclin B1. Oncogene2002;21(54):8282–92 doi 10.1038/sj.onc.1206011. [PubMed: 12447691]

55. Schoffski P, Blay JY, De Greve J, Brain E, Machiels JP, Soria JC, et al. Multicentric parallel phase II trial of the polo-like kinase 1 inhibitor BI 2536 in patients with advanced head and neck cancer, breast cancer, ovarian cancer, soft tissue sarcoma and melanoma. The first protocol of the European Organization for Research and Treatment of Cancer (EORTC) Network Of Core Institutes (NOCI). Eur J Cancer2010;46(12):2206–15 doi 10.1016/j.ejca.2010.03.039. [PubMed: 20471824]

56. Casey SC, Tong L, Li Y, Do R, Walz S, Fitzgerald KN, et al. MYC regulates the antitumor immune response through CD47 and PD-L1. Science2016;352(6282):227–31 doi 10.1126/science.aac9935. [PubMed: 26966191]

57. Kortlever RM, Sodir NM, Wilson CH, Burkhart DL, Pellegrinet L, Brown Swigart L, et al. Myc Cooperates with Ras by Programming Inflammation and Immune Suppression. Cell2017;171(6):1301–15e14 doi 10.1016/j.cell.2017.11.013. [PubMed: 29195074]

58. Han H, Jain AD, Truica MI, Izquierdo-Ferrer J, Anker JF, Lysy B, et al. Small-Molecule MYC Inhibitors Suppress Tumor Growth and Enhance Immunotherapy. Cancer cell2019;36(5):483–97e15 doi 10.1016/j.ccell.2019.10.001. [PubMed: 31679823]

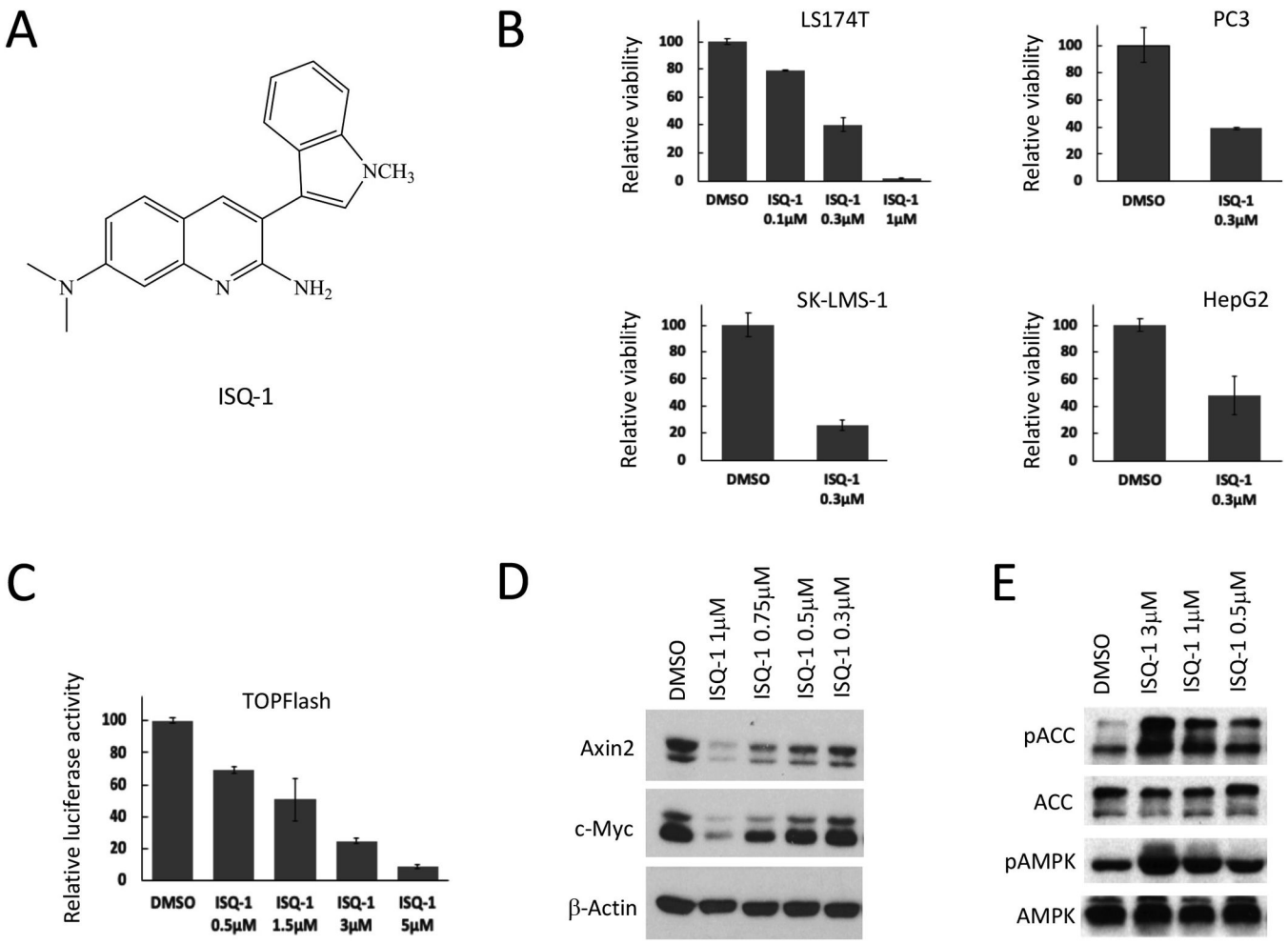


**Figure 1. Identification of indole-substituted quinolines as Wnt inhibitors and AMPK activators.**

**A**. Structure of ISQ-1. **B**. ISQ-1 inhibited proliferation of colon cancer cell line LS174T, prostate cancer cell line PC-3, sarcoma cell line SK-LMS-1 and liver cancer cell line HepG2 at nanomolar concentrations. Cells were treated with ISQ-1 at indicated concentrations for 5 days and counted. **C** and **D**. ISQ-1 inhibited TOPFlash Wnt reporter and Wnt signaling target genes c-Myc and axin2. Cells stably expressing TOPFlash Wnt reporter were treated for 24 hours and luciferase luminescence was analyzed (C). **E**. ISQ-1 activated AMPK and increased AMPK substrate ACC phosphorylation in LS174T cells.

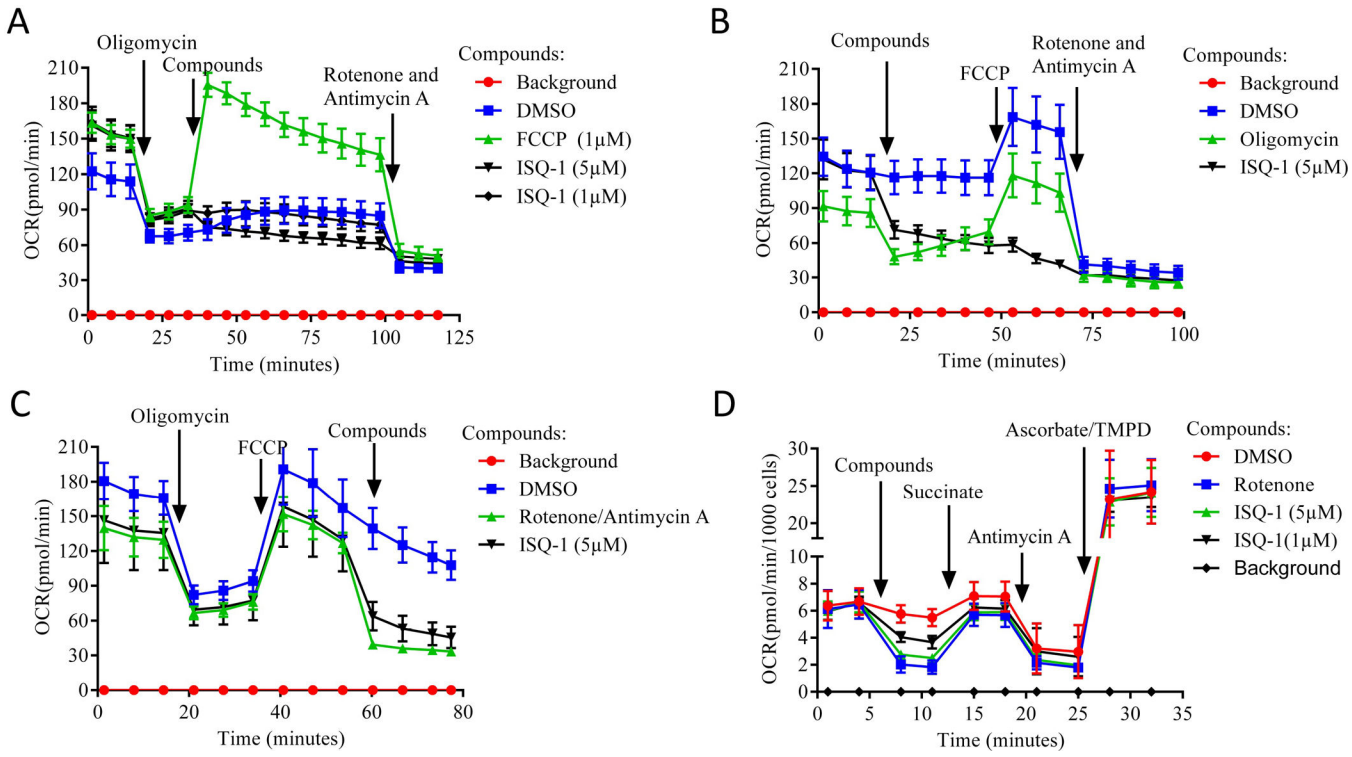


**Figure 2. ISQ-1 inhibited mitochondrial ETC (electron transport chain) complex I in LS174T cells.**

**A**. Seahorse assay. A classic uncoupler FCCP was replaced with ISQ-1 or DMSO. ISQ-1, unlike FCCP, failed to increase OCR and was not an uncoupler. **B**. Seahorse assay. ETC complex V (ATPase) inhibitor oligomycin was replaced with ISQ-1 or DMSO. OCR could not be rescued by the addition of FCCP in ISQ-1 treatment compared with oligomycin treatment, indicating that ISQ-1 did not inhibit ETC complex V. **C**. Seahorse assay. ETC complex complexes I/III inhibitors rotenone/antimycin were replaced with ISQ-1 or DMSO. ISQ-1 showed similar inhibitory effects on OCR compared with rotenone/antimycin, suggesting that ISQ-1 inhibited ETC complex I or III. **D**. Mitochondrial ETC complex activity measurements using PMP-permeabilized cells. PMP selectively disrupted cell membrane but left mitochondrial membrane intact. ISQ-1 inhibited OCR to a similar extent with rotenone, a complex I inhibitor. This inhibition was bypassed by adding the complex II substrate succinate, showing that ISQ-1 inhibited ETC complex I.

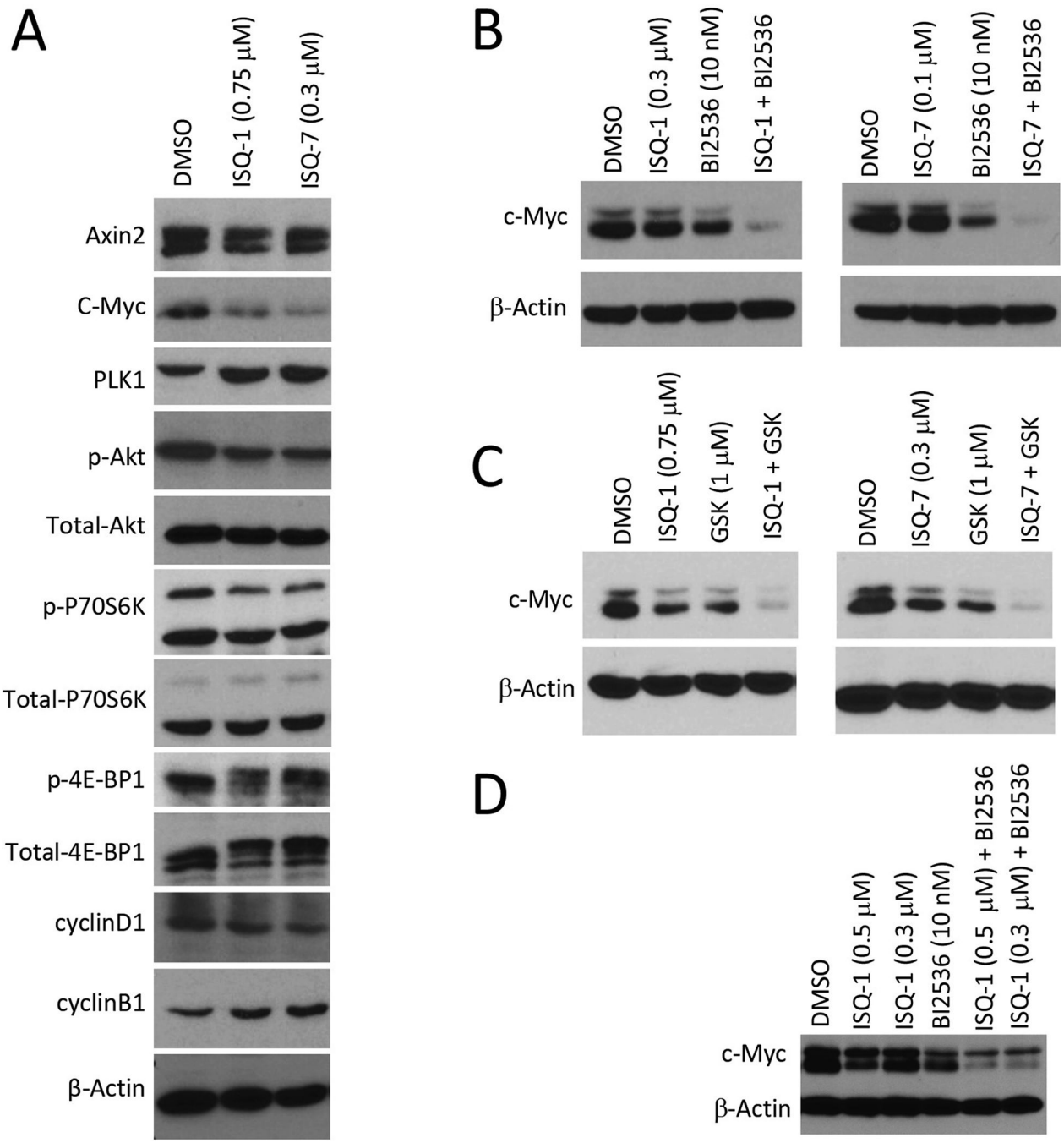


**Figure 3. Combinational effects of ISQs and Plk1 inhibitors on c-Myc expression after 24 hours treatment.**

**A**. Effects of ISQ-1 and ISQ-7 on cell signaling pathways in LS174T colon cells. A key cell cycle regulator Plk1 was induced upon drug treatment. **B**. Combination of ISQ-1 or ISQ-7 with Plk1 inhibitor BI2536 resulted in enhanced depletion of c-Myc in LS174T cells. **C**. Combination of ISQ-1 or ISQ-7 with Plk1 inhibitor GSK461364 resulted in enhanced depletion of c-Myc in LS174T cells. **D**. Combination of ISQ-1 with Plk1 inhibitor BI2536 resulted in enhanced depletion of c-Myc in prostate cancer PC3 cells.

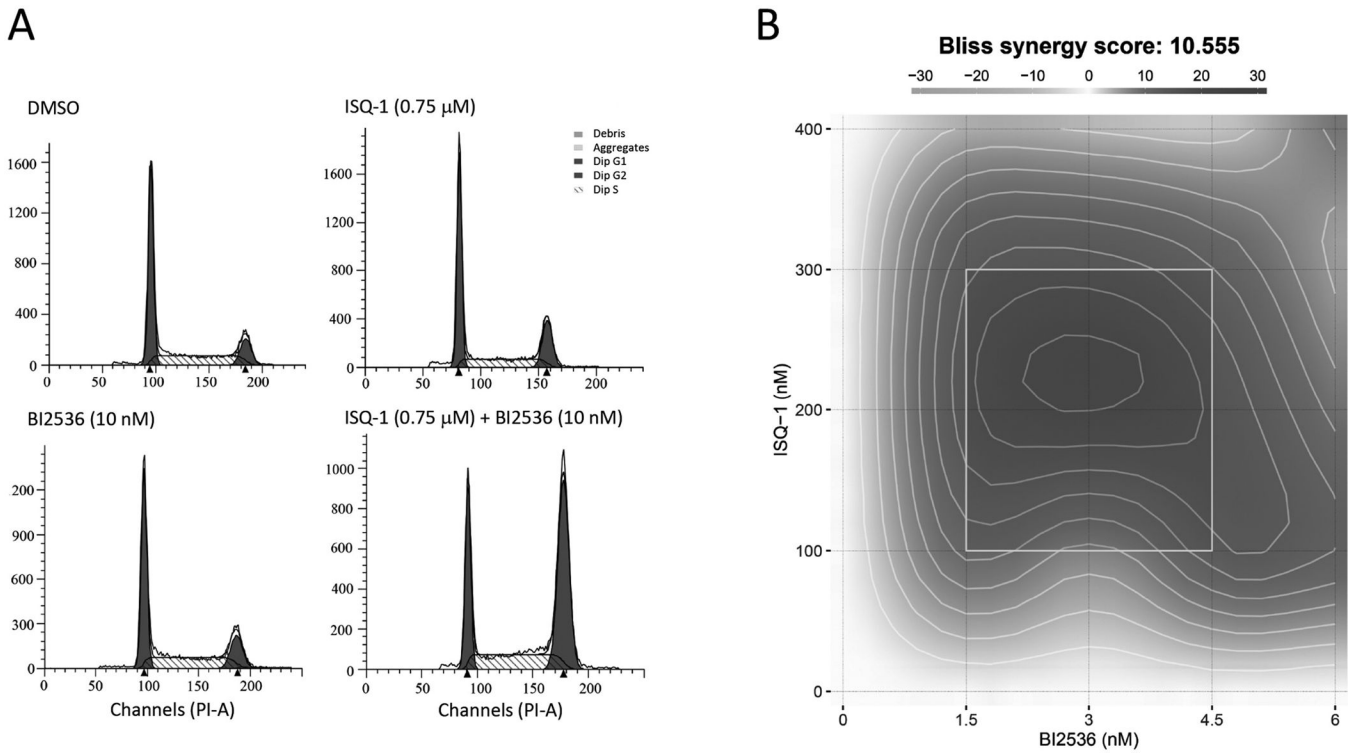


**Figure 4. Synergistic effects of ISQ-1 and BI2536 on colon cancer cell proliferation.**

**A**. ISQ-1 and BI2536 collectively inhibited cell cycle progression of LS174T colon cancer cells after 24 hours treatment. **B**. ISQ-1 and BI2536 synergistically inhibited the proliferation of LS174T cells. Synergy scores were determined using SynergyFinder with Bliss as a reference model.

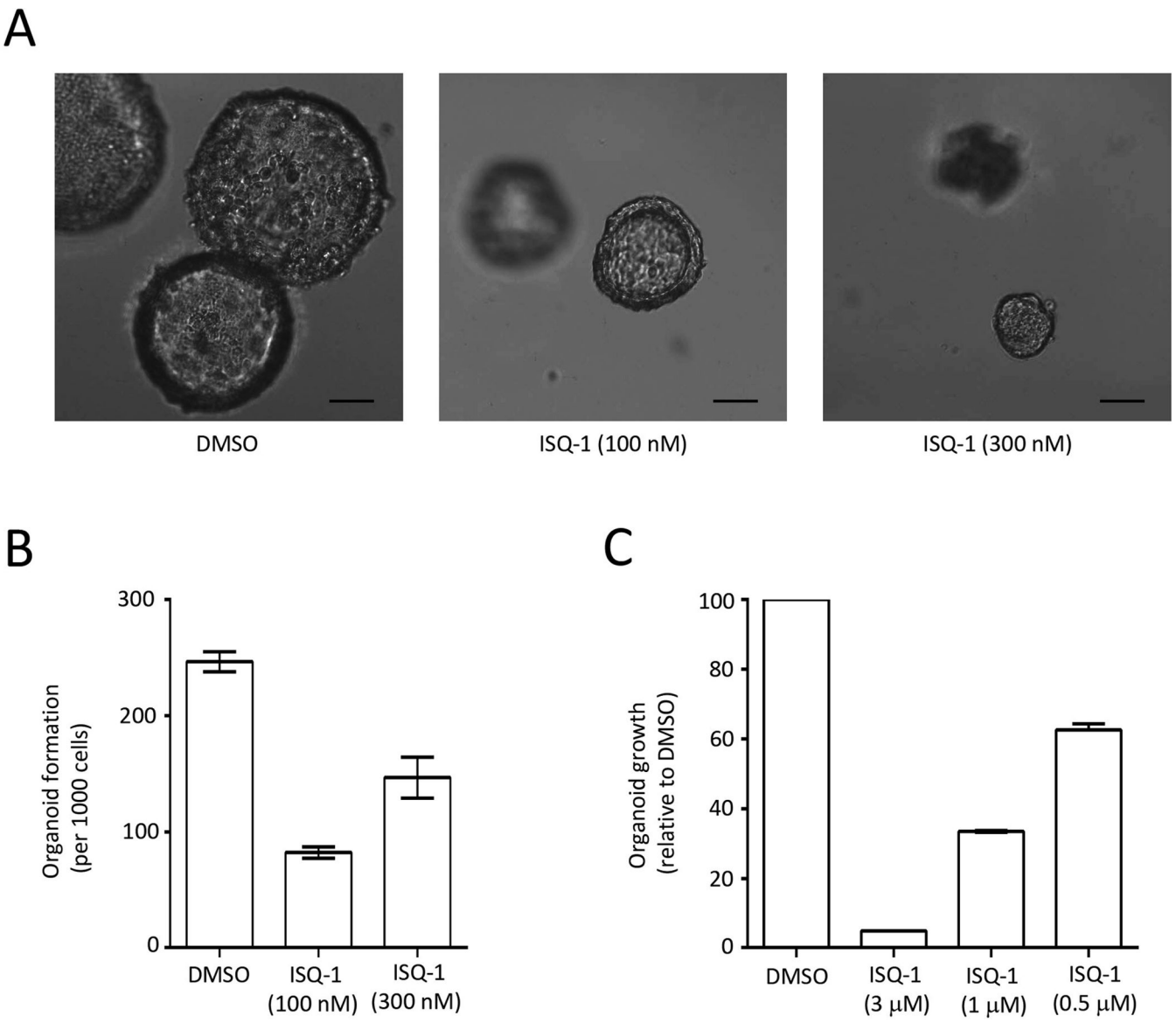


**Figure 5. ISQ-1 inhibited mouse colon cancer organoids from Apc$^{f/+}$/Kras$^{LSL-G12D}$/Villin-Cre mouse model.**

**A**. Colony formation of colon cancer organoids from single cells after DMSO or ISQ-1 treatment at day 7. Scale bar, 50 μm. **B**. ISQ-1 inhibited organoid colony formation. Total number of organoids formed from single cells in the presence of DMSO or ISQ-1 at day 7 was quantified. **C**. ISQ-1 inhibited organoid growth after 3-day treatment. ISQ-1 or DMSO were added after organoids were formed from single cells. Organoid viability was measured using CellTiter-Glo® 3D Cell Viability Assay (Promega).

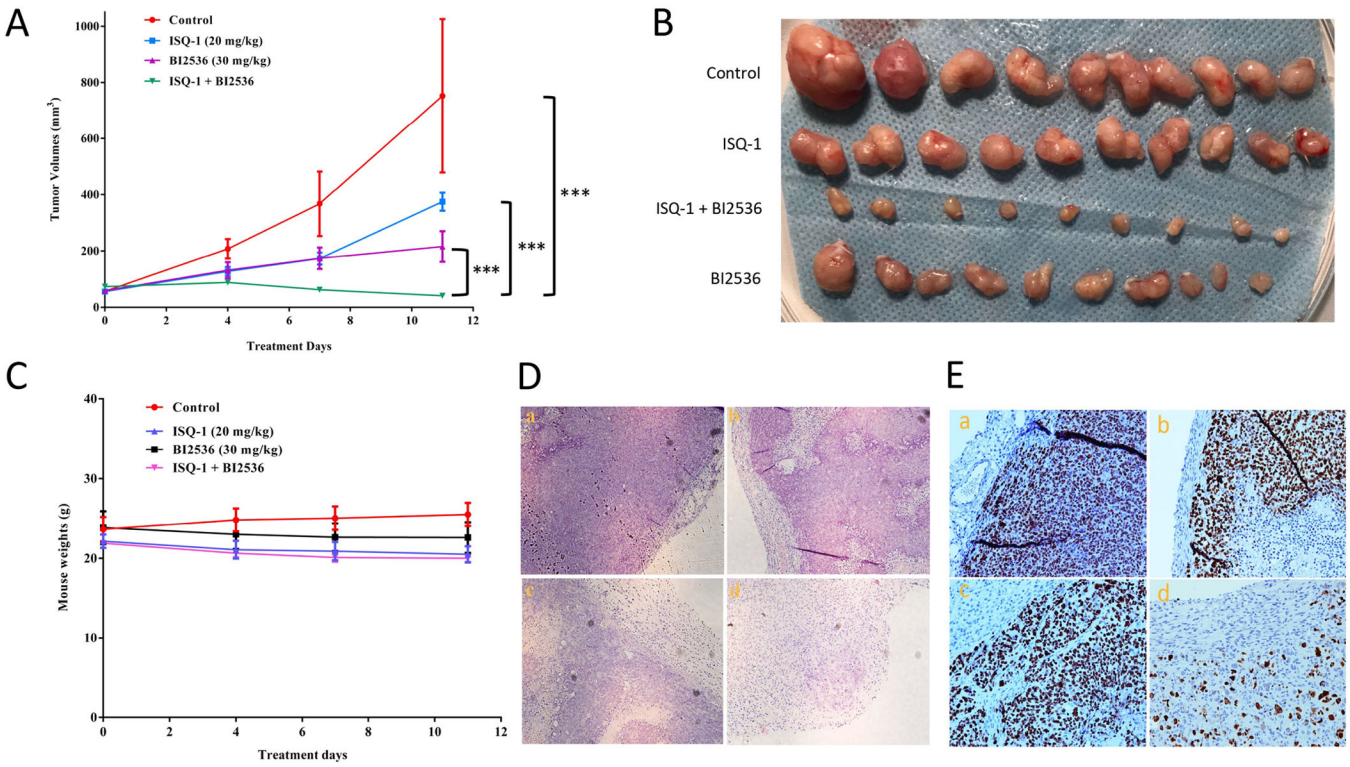


**Figure 6. ISQ-1 and the Plk1 inhibitor BI2536 synergistically inhibited colon cancer cell xenografts *in vivo*.**

**A** and **B**. ISQ-1 (20 mg/kg/day) and BI2536 (30 mg/kg twice a week) synergistically induced regression of LS174T colon cancer cell xenografts in nude mice. ***$P <$ 0.001, analysis of variance (ANOVA) followed by Tukey's HSD test. **C**. Mouse weight measurements following various treatments. **D**. H&E staining of tumors (a: control; b: ISQ-1; c: BI2536; d: ISQ-1 + BI2536). **E**. ISQ-1 and BI2536 collectively inhibited Ki-67 expression in LS174T xenografted tumors (a: control; b: ISQ-1; c: BI2536; d: ISQ-1 + BI2536).